Sensors and Actuators B 259 (2018) 505–513

Contents lists available at ScienceDirect

Sensors and Actuators B: Chemical

journal homepage: www.elsevier.com/locate/snb

The room temperature gas sensor based on Polyaniline@flower-like WO_3 nanocomposites and flexible PET substrate for NH_3 detection

Siqi Li, Pengfei Lin, Liupeng Zhao, Chong Wang, Deye Liu, Fangmeng Liu*, Peng Sun, Xishuang Liang, Fengmin Liu, Xu Yan, Yuan Gao, Geyu Lu*

State Key Laboratory on Integrated Optoelectronics, College of Electronic Science and Engineering, Jilin University, 2699 Qianjin Street, Changchun 130012, People's Republic of China

ARTICLE INFO

Article history:
Received 14 August 2017
Received in revised form 18 October 2017
Accepted 17 November 2017
Available online 21 November 2017

Keywords:
Room temperature
NH_3 sensor
PANI
Flower-like WO_3
Flexible PET substrate

ABSTRACT

The Polyaniline (PANI)@flower-like tungsten oxide (WO_3) nanocomposites with different mole percentages of flower-like WO_3 (2–50%) were successfully synthesized by using a facile in situ chemical oxidation polymerization method and were loaded on flexible polyethylene terephthalate (PET) substrate to fabricate NH_3 sensors operating at room temperature. The morphology, nanostructures and thermal degradation behavior of the as-obtained sensing materials were measured and characterized utilizing SEM, TEM, FTIR, XRD and TG. Gas-sensing performances of fabricated sensors were tested and results indicated that the sensor with PANI@10 mol% flower-like WO_3 exhibited the highest response value at approximately 20.1–100 ppm NH_3 at room temperature, which is more than 6 times higher than that of pure PANI. Notably, the lowest detection limit of 500 ppb to NH_3 was obtained at room temperature. Furthermore, the present sensor also showed rapid response and recovery rates of 13 s and 49 s, good repeatability, selectivity, and slight humidity effects to 10 ppm NH_3 at room temperature. Moreover, the gas sensing mechanisms of PANI and nanocomposites were also discussed in detail. The enhanced sensing characteristics of nanocomposites were related to the morphology structure and *p-n* heterojuction between PANI and flower-like WO_3.

1. Introduction

Ammonia (NH_3), one of the hazardous gases, released by most chemical industries and agricultural production, has characteristics of colorless but horribly irritating scent and strongly corrosive to eyes and respiratory organs [1]. According to the national standard of Workplace Hazardous Occupational Exposure Limits, the maximum allowable concentration of NH_3 in the workshop is 40 ppm. Hence, development of NH_3 gas sensor with high gas sensing performance including high sensitivity, low detection limit and room temperature detection has essential practical significance.

In the past several decades, various types of NH_3 sensors have been developed, such as oxide semiconductor type gas sensors based on SnO_2 [2], In_2O_3 [3], Fe_2O_3 [4] WO_3 [5] and solid state electrolyte type gas sensor using Cr_2O_3 [6], $Ni_3V_2O_8$ [7], TiO_2@WO_3 [8]. However, the sensors employed in these techniques had the disadvantage of high temperature operation and caused the higher energy consumption [9]. To address such limitations, Sensors based on conductive polymer and metal oxide semi-conductor composite materials, which not only retain the advantages of high sensitivity of metal oxide semi-conductor but also possess low detection temperature and excellent selectivity of conductive polymer, have been demonstrated to be effective method for room temperature detection of NH_3. On the one hand, the sensors have much lower initial resistance owing to the wide conducting channels provided by conductive polymer. On the other hand, the formation of heterojunctions between conductive polymer and oxide semi-conductor has a great influence on the sensing behavior [10]. Li et al. fabricated Fe_2O_3/PANI sensor by dip-coating water-dispersible polyaniline to Fe_2O_3 nanosheets. It was revealed that the Fe_2O_3/PANI nanocomposite achieved high sensitivity and excellent selectivity towards NH_3 at room temperature [11]. Wang et al. reported a room-temperature NH_3 gas sensor based on CeO_2 NPs uniformly coated by cross-linked PANI, exhibited the sensing characteristics of high response and great long-term stability [12]. Nie et al. synthesized In_2O_3/PANI via in situ polymerization PANI to In_2O_3 nanofibers to detect NH_3 in a wider concentration range at room temperature [13].

Tungsten oxide (WO_3) as a typical n-type semi-conductor has good characteristics of relatively low resistance, easily synthesized, low preparation cost and environmentally friendly, was widely used for gas sensing materials [14]. Among the conductive poly-

* Corresponding authors.
E-mail addresses: lfm198705@126.com (F. Liu), lugy@jlu.edu.cn (G. Lu).

https://doi.org/10.1016/j.snb.2017.11.081
0925-4005/

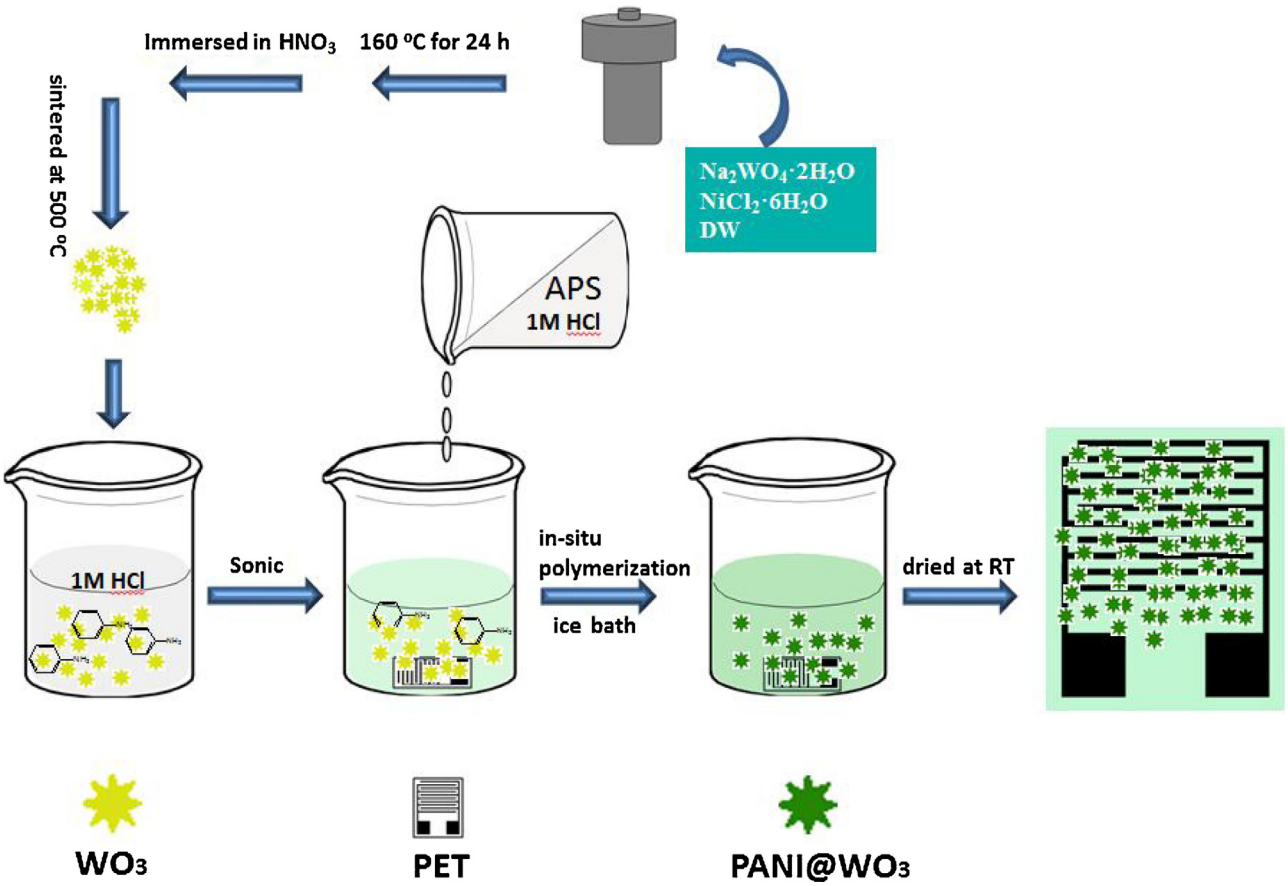

Fig. 1. Schematic illustration of the preparation of PANI@flower-like WO_3 nanocomposite films.

mers, polyaniline (PANI) acquires the most attention for its high electrical conductivity, easy to synthesis, low cost, good environmental stability and was sensitive to kinds of gases at room temperature [13,15]. Nano-scale polyaniline has the unique electrical properties owing to the high surface-to-volume ratios and small dimensions, which facilitates enhanced interaction between sensing materials and target gas for high sensitivity and enable fast adsorption/desorption kinetics for target gas on the materials for a rapid response and recovery [16]. Polyaniline nanofibers (PANINF) and polyaniline nanotubes (PANINT) have significant higher conductivity than that of conventional granular polyaniline, because of their one-dimensional nanostructure has longer polymer conjugated backbone [17,18]. However, rarely studies have reported on NH_3 detection using special structure semi-conductors and one-dimensional PANI conductive polymer composite as the sensing materials detect at room temperature.

In this work, for the first time, a series of PANI@flower-like WO_3 nanocomposites were synthesized through a facile in situ chemical oxidation polymerization method and were loaded on flexible PET substrates to fabricate NH_3 sensors operating at room temperature. The assembled gas sensor exhibited high sensitivity, rapid response and recovery rates, low detection limit, good repeatability, good selectivity and slightly humidity effect to NH_3 at room temperature. Moreover, the related mechanism underlying gas sensing was also discussed in detail.

2. Experiment

2.1. Synthesis of flower-like WO_3 material

All of the chemical reagents involved in the experiment were analytical grade and directly used without any further purification. Flower-like WO_3 assembled with nanosheets were synthesized as reported [19]. The typical synthesis procedure was described as follows:1.3 g $Na_2WO_4{\cdot}2H_2O$ and 0.95 g $NiCl_2{\cdot}6H_2O$ were dissolved in 20 mL of distilled water under vigorous stirring for 30 min, respectively, and were mixed under continuous stirring for another 10 min to produce uniform green solution. Then, the above-obtained mixture solution was transferred into a Teflon-lined stainless steel autoclave and maintained at 160 °C for 24 h. Subsequently, the product was washed with deionized water and ethanol alternately for several times, and dried at drying oven of 80 °C for 8 h to get green power product. Then, 0.08 g above obtained sample was immersed in specific concentration of HNO_3 solution, following the product was turned gradually from green to yellow under continuous stirring. Finally, the yellow as-prepared product obtained by centrifugation, washing and drying was sintered at 500 °C to obtain flower-like WO_3 nanostructure material.

2.2. Synthesis of HCl doped PANI nanofibers and PANI@flower-like WO_3 nanocomposite films

Polyaniline nanofibers were synthesized using aniline monomers by a facile chemical oxidative polymerization method. Briefly, 0.2 mmol aniline (distilled before use) and different mole percentages of flower-like WO_3 (mol% = 0, 2, 5, 10, 20 and 50) was added into 20 mL of 1 M HCl solution and treated with ultrasonic wave for 30 min. Meanwhile, 0.2 mmol ammonium persulfate (APS) was disolved in certain amount of HCl solution under vigorous stirring for 30 min to get APS/HCl solution and precooled at ice bath. Then, APS/HCl solution was added into above obtained solution, subsequently, a piece of PET film vaporized with gold interdigital electrode (The flexible PET substrate with length × width × thickness of 1cm × 0.8 cm × 125 um was

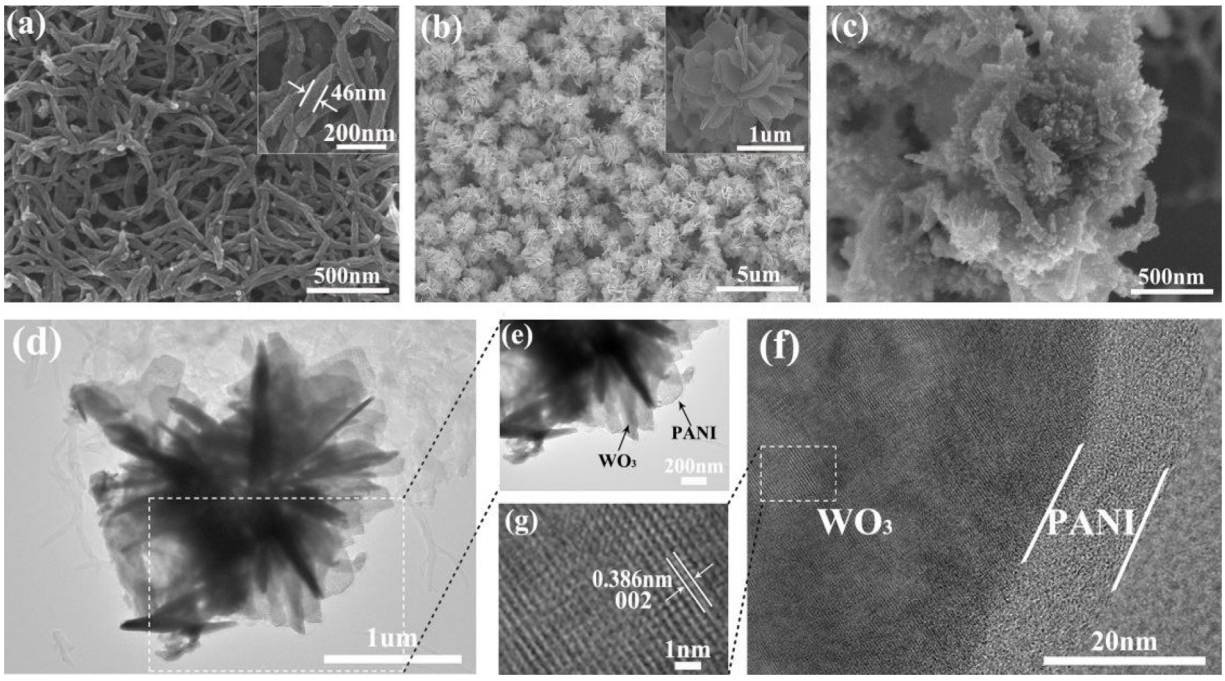

Fig. 2. FESEM images of (a) PANI; (b) flower-like WO_3; (c) High-magnification SEM images of PAW10 hybrid; (d, e) TEM images of PAW10 hybrid; (f, g) HRTEM images of PAW10 hybrid.

purchased from Dawan Plastic Electronics Company; The PET film is at optical grade and the transmittance is higher than 90%. The thickness, length and width of gold inter-digital electrode vaporized on PET substrate are 100 nm, 8.5 mm and 6 mm respectively. The width of fingers is 0.2 mm and spacing between fingers of inter-digital electrodes is 0.3 mm) was immersed in the mixed solution and the polymerization reaction process was kept for 2 h under ice bath condition. The schematic illustration of synthetic process was depicted in Fig. 1. The polymerized products were collected by high speed centrifugal separation and washed for several times with distilled water and absolute ethanol and dried at 80 °C for further characterization. The resultant PANI@flower-like WO_3 nanocomposites were denoted as PANI, PAW2, PAW5, PAW10, PAW20 and PAW50, respectively. The obtained films were washed with distilled water to remove the impurities and dried at room temperature.

2.3. Characterization

Field emission scanning electron microscopy (FESEM, JEOL JSM-7500F, operated at 5 kV) was used to investigate the morphology and microstructure of prepared samples. Transmission electron microscopy (TEM) image and high-resolution transmission electron microscopy (HRTEM) image of samples were performed using JEM 2100F microscope with an acceleration voltage of 200 kV. The crystallographic information of products was recorded using X-ray diffraction (XRD, Rigaku D/max-2550) with Cu-Kαradiation (λ = 0.15406 nm) within the range of 20–80° (2θ). Fourier Transform Infrared spectroscopy (FTIR) analysis of samples was tested in the wavenumber range of 4000–500 cm^{-1} with a PE-400 spectrometer at room temperature with the ATR plugin. Thermo gravimetric (TG) analysis of samples was carried out using NETZSCHSTA449 F3 thermal analyzer in the temperature range of 30–800 °C at heating rate of 10 °C/min under air atmosphere.

2.4. Gas-sensing measurements of fabricated sensors

The gas-sensing measurements of fabricated sensors were carried out using a conventional static test system under laboratory conditions (25 ± 5% RH, 20 ± 1 °C) according to our previous reported [20], which can provide real-time data output signals. The response S of fabricated sensor is defined as the following equation:

$$S = \frac{R_g}{R_a}$$

Where, R_a and R_g represent the resistances of the sensor in air and in target gas, respectively. The response and recovery times are defined as the time required for the sensor to achieve 90% of stable resistance when the fabricated sensor was exposed to the target gas and air.

3. Results and discussion

3.1. Morphological, structural and thermal stable characteristics

The morphologies of the pure PANI, flower-like WO_3 and PANI@flower-like WO_3 nanocomposites were observed through FESEM as shown in Fig. 2. The morphologies of PANI were nanofibers structure with the diameter of about 46 um (Fig. 2a). No other morphologies were observed, indicating the good uniformity and dispersibility of the nanostructures. From the FESEM image of the flower-like WO_3 in Fig. 2b, the flower-like WO_3 were assembled by many smooth nanosheets can be observed clearly. These nanosheets possess a thickness of approximate 50 nm. As can be seen from the PAW10 hybrid in Fig. 2c, the PANI grown on the surface of flower-like WO_3, leading the surface of flower-like WO_3 to rough. TEM images further revealed the structure and morphologies of PAW10 hybrid. As shown in Fig. 2(d, e), the translucent PANI was wrapped on the surface of flower-like WO_3 is identical to that in the SEM result. Fig. 2(f and g) displayed high-resolution TEM (HRTEM) images of PAW10 hybrid. The amorphous PANI was evenly coated on the surface of flower-like WO_3. Moreover, the value of distance between the adjacent lattice planes is 0.386 nm corresponding to (002) planes of monoclinic flower-like WO_3 were clearly observed in Fig. 2g. The morphologies of the PANI@flower-like WO_3 composites with different additions of flower-like WO_3

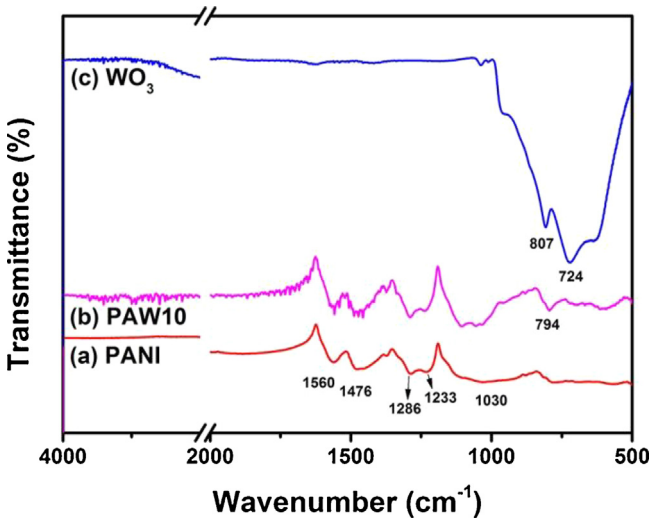

Fig. 3. FTIR spectra of (a) PANI; (b) PAW10 hybrid; (c) flower-like WO_3.

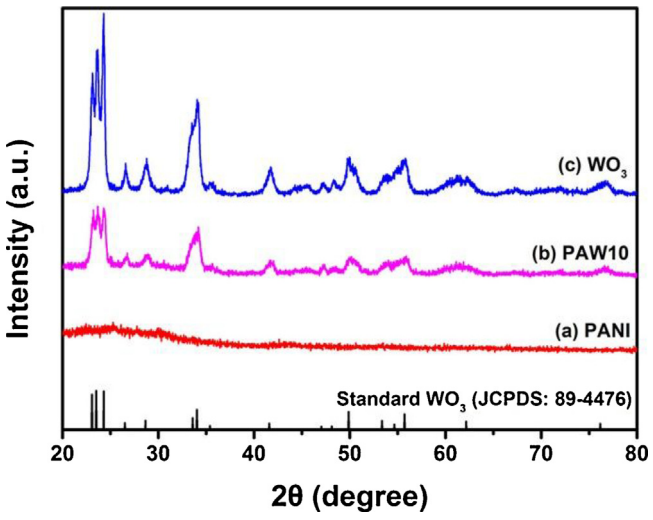

Fig. 4. XRD patterns of (a) PANI; (b) PAW10 hybrid; (c) flower-like WO_3.

(mol%) were shown in Fig. S1 (as seen in Supporting information). It was found that an obvious distinction of heterointerface between PANI and flower-like WO_3 existed among PAW2 hybrid, PAW5 hybrid, PAW20 hybrid, and PAW50 hybrid. Fig. S1a, b showed amount of uncomplexed PANI and thicker polyaniline layer combined to flower-like WO_3 than PAW20 hybrid, and PAW50 hybrid. Inversely, Fig. S1c, d depicted the existence of flower-like WO_3 incompletely coated with PANI.

FTIR spectroscopy was conducted to characterize and confirm the chemical structure of pure PANI, flower-like WO_3 and the PAW10 hybrid. Fig. 3 shows the typical FTIR spectrum of samples within the wavenumber range of 4000–500 cm^{-1}. The peaks assigned at 1560, 1476, 1286, 1233 and 1030 cm^{-1} were ascribed to the main characteristic absorption peaks of polyaniline [21]. In detail, the peak located at 1560 cm^{-1} was associated with N=Q=N stretching vibration of the quinoid structure, whereas the signal at 1476 cm^{-1} was identified to N—B—N absorption vibration of benzenoid structure. The absorption bands assigned to the stretching vibration of C—N and C=C were located at 1286 and 1233 cm^{-1} [22,23]. The characteristic band located at 724 and 807 cm^{-1} was attributed to W—O—W stretching vibration of WO_3 (Fig. 3c) [24]. The images shown in Fig. 3b revealed the characteristic peaks of PAW10 hybrid were shifted to higher wavenumbers at about 1566, 1480, 1289, 1237 cm^{-1}, suggesting an interaction between PANI and flower-like WO_3, which indicating a successful combination of PANI and flower-like WO_3.

The crystal structure of pure PANI, flower-like WO_3 and PAW10 hybrid was determined by XRD measurement. The XRD patterns of pristine PANI showed a broad and week diffraction peak at about $2\theta = 20–30^{\circ}$, which indicated the amorphous phase structure of sample (Fig. 4a) [23]. The XRD pattern of pure flower-like WO_3 is shown in Fig. 4c, and all the specific diffraction peaks were matched well with those from the standard values of JCPDS card No.89-4476, which is indexed to the monoclinic structures of flower-like WO_3. No other redundant diffraction peak or impurity phase was observed, indicating the phase purity of formation flower-like WO_3. From the XRD pattern of PAW10 hybrid showed in Fig. 4b, it can clearly observe that the main specific diffraction peaks of WO_3 were also detected. Interestingly, the degree of diffraction peaks became weaker than that of the pure flower-like WO_3, which might be attributed to the growth of PANI on the surface of flower-like WO_3. The result demonstrates the coexistence of PANI and flower-like WO_3 by in situ polymerization.

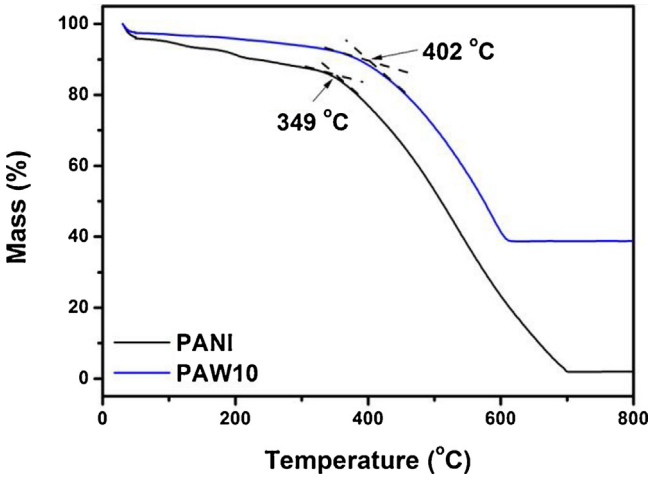

Fig. 5. TG curves of (a) PANI; (b) PAW10 hybrid.

The Thermogravimetric (TG) analysis of the pure PANI and PAW10 hybrid was measured to investigate the thermal stability of samples. As shown in Fig. 5, the TG curves of pure PANI and PAW10 hybrid showed a little mass loss before 100 °C due to the releasing of surface-absorbed water molecules. The curves demonstrated that the mass loss of PAW10 hybrid was less than that of pristine PANI [25]. For pure PANI, the gradual weight loss between 100 and 349 °C was because of the elimination of dopant HCl of acid PANI and the major weight loss above 349 °C was assigned to the decomposition of PANI [26]. Almost no residual products were observed when the temperature rises to 700 °C for the pure PANI in air atmosphere. The PAW10 hybrid exhibited a relative slower mass loss than that of pure PANI, and the maximum thermal degradation behavior took place at above 402 °C. The residual amount of 38.8% was remained when the temperature increased above 615 °C. These confirmed that the incorporation of flower-like WO_3 and the interfaction between PANI and flower-like WO_3 obviously enhanced the thermal stability of PAW10 hybrid, considering the PANI@ flower-like WO_3 as the promising sensing material.

3.2. Gas sensing properties

The prepared pure PANI, flower-like WO_3 and PANI@ flower-like WO_3 hybrid sensing materials were assembled as flexible devices based on PET substrates, and the gas sensing properties were inves-

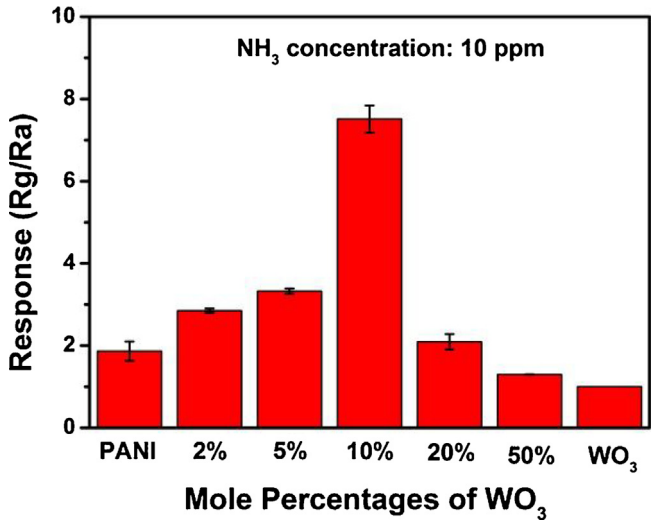

Fig. 6. The effect of mole percentages of WO_3 on the response of sensor.

tigated at room temperature, respectively. Fig. 6 represents the responses of PANI and PANI@flower-like WO_3 flexible films with different additions ratio of flower-like WO_3 (mol%) to 10 ppm NH_3 at room temperature. It was found that the pure flower-like WO_3 had no obvious sensitive signal to 10 ppm NH_3 at room temperature, and the response value of pure PANI was approximately 1.8. However, the response of the sensor based on PANI@flower-like WO_3 exhibited a significant "peak" shape with the trend of "increase-maximum-decrease" to 10 ppm NH_3 at room temperature with the increasing in the amount of flower-like WO_3 addition and the highest response value of 7.5 was obtained when the addition amount of flower-like WO_3 was 10 mol%. The phenomenon for the properties of PAW20 hybrid and PAW50 hybrid compared poor to PAW10 hybrid was mainly attributed to the following two aspects: First, for PAW20 hybrid and PAW50 hybrid (Fig. S1c, d) the surplus addition of flower-like WO_3 made PANI insufficient to completely cover the surface of flower-like WO_3 and certain amount of NH_3 was absorbed on the surface of flower-like WO_3 which would not improve the sensitive properties to NH_3. On the other hand, a large amount of electrons provided by excess flower-like WO_3 made the depletion area thicker at the heterointerface between PANI and flower-like WO_3, which would reduce the sensitivity markedly. Therefore, addition of excess flower-like WO_3 was unfavorable to enhance the response of PANI@flower-like WO_3 to NH_3.

Fig. 7a depicts the response transients of the flexible devices based on pure PANI, flower-like WO_3 and PAW10 hybrid to different concentrations of NH_3 (0.5–100 ppm) at room temperature. The gas responses of fabricated sensors increased with increasing NH_3 concentration from 0.5 to 100 ppm. The PAW10 hybrid achieved the highest response of 20.1–100 ppm NH_3, which is more than 6 times higher than that of pure PANI, indicating that PAW10 hybrid could be used as promising materials for NH_3 gas detection. Table 1 shows the comparisons for the sensing properties of PAW10 hybrid and previously reported devices were shown in Table 1. Quite clearly, the present sensor based on PAW10 hybrid exhibited the best sensing performance to NH_3 at room temperature comparing with previously reported devices. Hence, combined PANI with flower-like WO_3 could be an effective approach for improving the sensing response of sensors to the NH_3. The response and recovery characteristics of PAW10 hybrid to 10 ppm NH_3 were further investigated at room temperature shown in Fig. 7b. The response and recovery times were approximately 13 and 49 s to 10 ppm NH_3, respectively. Incidentally, the original response value of the gas sensor recovered to the original response value after exposure to 10 ppm NH_3 gas, indicating the response and recovery characteristic to 10 ppm NH_3 exhibited good reproducibility in the process of five continues cycles (Inset of Fig. 7b).

Meanwhile, as an important index of sensing performance parameters, the selectivity of sensors based on pure PANI and PAW10 hybrid was measured with various testing gases of 10 ppm, including NH_3, methane, ethanol, acetone, toluene, formaldehyde, H_2 and CO at room temperature and corresponding results were shown in Fig. 8. It can be clearly seen that the sensor utilizing PAW10 hybrid performed the highest response value to NH_3 compared with any other test gases, and the enhanced degree of response to NH_3 as opposed to other gases was evidently better than that of pure PANI. Consequently, it concluded that the sensor based on PAW10 hybrid showed selectivity toward NH_3 against other gases at room temperature.

Furthermore, in order to investigate the effect of humidity on sensing performance, the performance of PAW10 hybrid to 10 ppm NH_3 were measured in different relative humidity conditions (20–98% RH) at room temperature, as illustrated in Fig. 9. Obviously, the response value of PAW10 hybrid to 10 ppm NH_3 displayed slight fluctuation in the examined relative humidity,

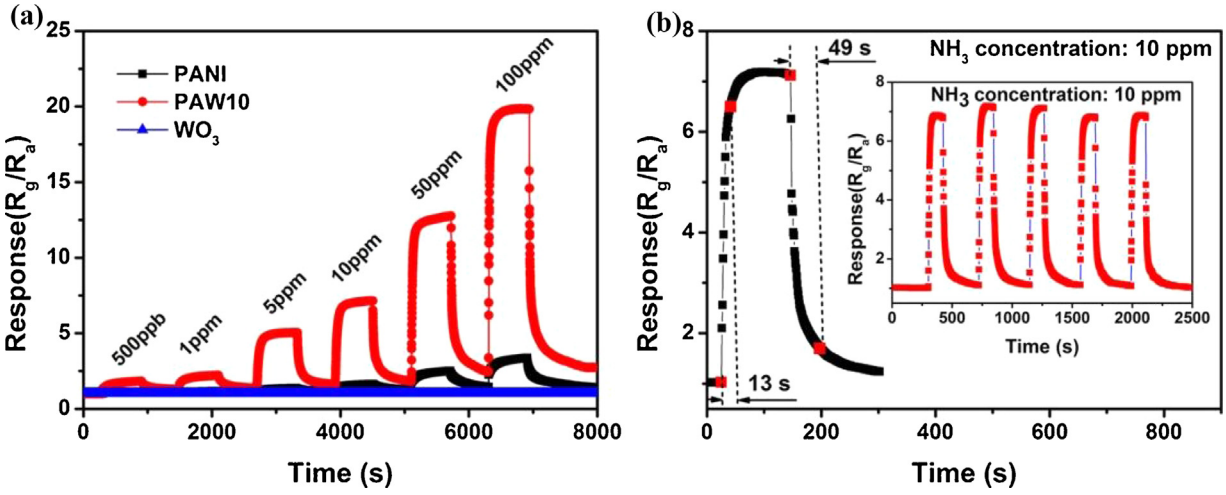

Fig. 7. (a) The response transients of the flexible devices based on pure PANI, flower-likeWO_3 and PAW10 hybrid to different concentrations of NH_3 at room temperature; (b) Dynamic response-recovery curves of PAW10 hybrid to 10 ppm NH_3 at room temperature.

Table 1
Comparison of sensing properties for the gas sensors based on PAW10 hybrid synthesized in this work and some other previously reported.

Materials	Gas	Conc. (ppm)	Temp. (°C)	The formula of response	Response	Ref.
PANI/WO_3	NH_3	100	RT	$S = R_g/R_a$	20.1	This work
PANI	NH_3	100	RT	$S = (R_g - R_a)/R_a \times 100\%$	96%	[30]
PANI/GO/ZnO	NH_3	300	RT	$S = (I_a - I_g)/I_g$	1.307	[27]
PANI/TiO_2/Au	NH_3	50	RT	$S = (R_g - R_a)/R_a \times 100\%$	123%	[31]
CSA-PANI/Fe_2O_3	NH_3	100	RT	$S = (R_g - R_a)/R_a \times 100\%$	72%	[32]
Pt-WO_3	NH_3	200	125	$S = R_a/R_g$	13.61	[20]
V-WO_3	NH_3	500	700	$S = R_a/R_g$	14	[33]
Ni_2O_3-WO_3	NH_3	200	250	$S = R_a/R_g$	13.5	[34]
PANI/Pd	NH_3	500	RT	$S = R_g/R_a$	21.9	[35]
PANI-WO_3	NH_3	100	RT	$S = (R_g - R_a)/R_a \times 100\%$	158%	[14]

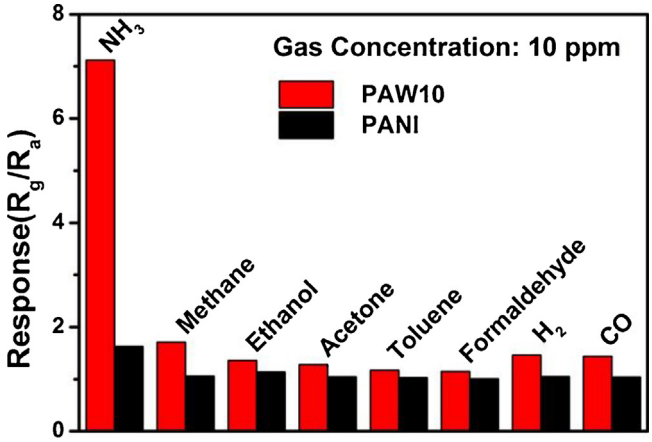

Fig. 8. The selectivity of sensors based on pure PANI and PAW10 hybrid to various testing gases of 10 ppm at room temperature.

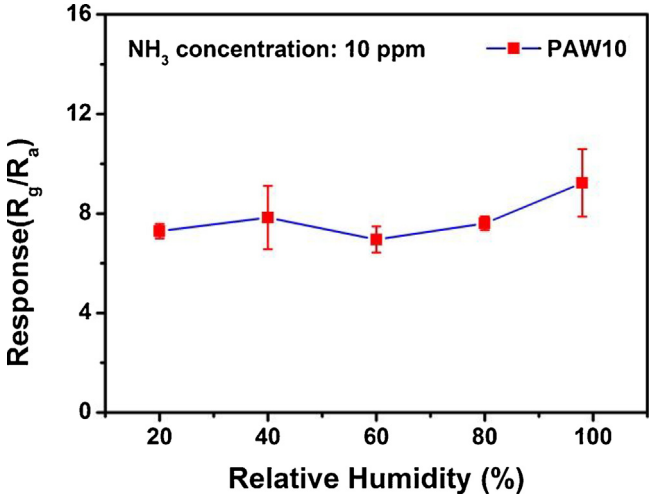

Fig. 9. The effect of relative humidity on the response of sensor utilizing PAW10 hybrid.

indicating the sensor displayed good moisture resistance at room temperature.

Additionally, the stability of the sensor based on PAW10 hybrid was measured to 10 ppm NH_3 for consecutive two weeks at room temperature. The responses of PAW10 hybrid to 10 ppm NH_3 were obtained every day and the result was presented in Fig. 10. In the first week, the response had obvious decline, which might be caused by the film aging and disappearance of instable adsorption sites [27]. Finally, the responses of PAW10 hybrid reached relative stable states (about 50% of initial responses). Therefore, the stability of sensors based on nanocomposites of conductive polymer and semiconductor oxide should be paid more attention.

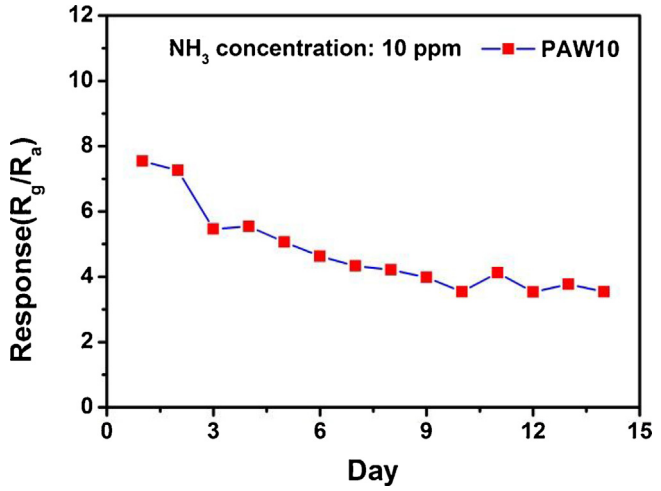

Fig. 10. Stability of Gas sensor based on PAW10 hybrid stored unencapsulated at room temperature for 15 days.

3.3. *Sensing mechanism of PANI and PANI@flower-like WO_3 hybrid to NH_3*

The most widely accepted sensing mechanism of pure PANI is related to the deprotonation/protonation process, depending on the acid/base environment as depicted in Fig. 11. When the sensor based on acidified PANI was exposed to NH_3 gas, NH_3 molecules withdrew the protons from acidified PANI, resulting PANI based on conductive emeraldine salt state reduced to intrinsic emeraldine base state, which lead to the increases of resistance [28]. On the contrary, when the sensor was placed in the air atmosphere, the reaction process was reversed and the resistance decreased. Additionally, as Fig. 7a showed, the response of the sensor utilizing PAW10 hybrid exhibited a significant improvement comparing with that of pure PANI and flower-like WO_3. The corresponding result could be explained by two aspects. First, according to the SEM image of Fig. 2c, the PAW10 hybrid was obtained by growing the PANI on the surface of flower-like WO_3, loose and porous structure was formed based on numerous of PAW10 hybrid. The structure with a larger specific surface area is conducive to adsorption and diffusion of more NH_3 gas molecules on the surface of PAW10 hybrid sensing material to improve the sensitivity. The other more important reason for enhancement of the sensitivity was attributed to the *p-n* heterojunction formed at the surface between p-type PANI and n-type flower-like WO_3 [12]. The acidified PANI provided a number of free holes in the valence band due to protonic acid doping and flower-like WO_3 as an n-type semiconductor showed a large amount of free electrons. When PANI nanofiber was cov-

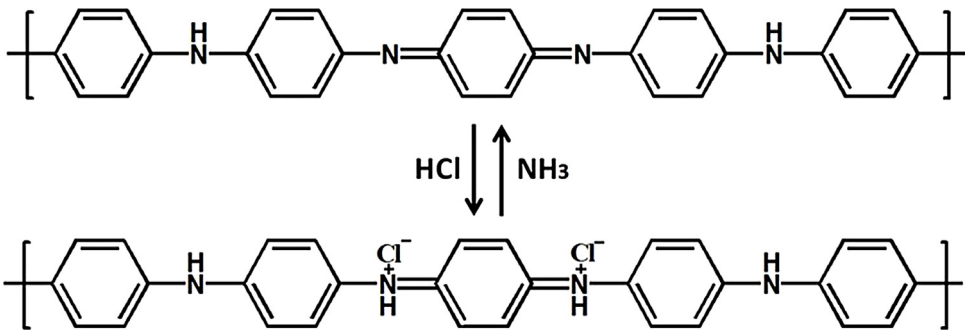

Fig. 11. Schematic illustration of the interaction of NH_3 gas with PANI.

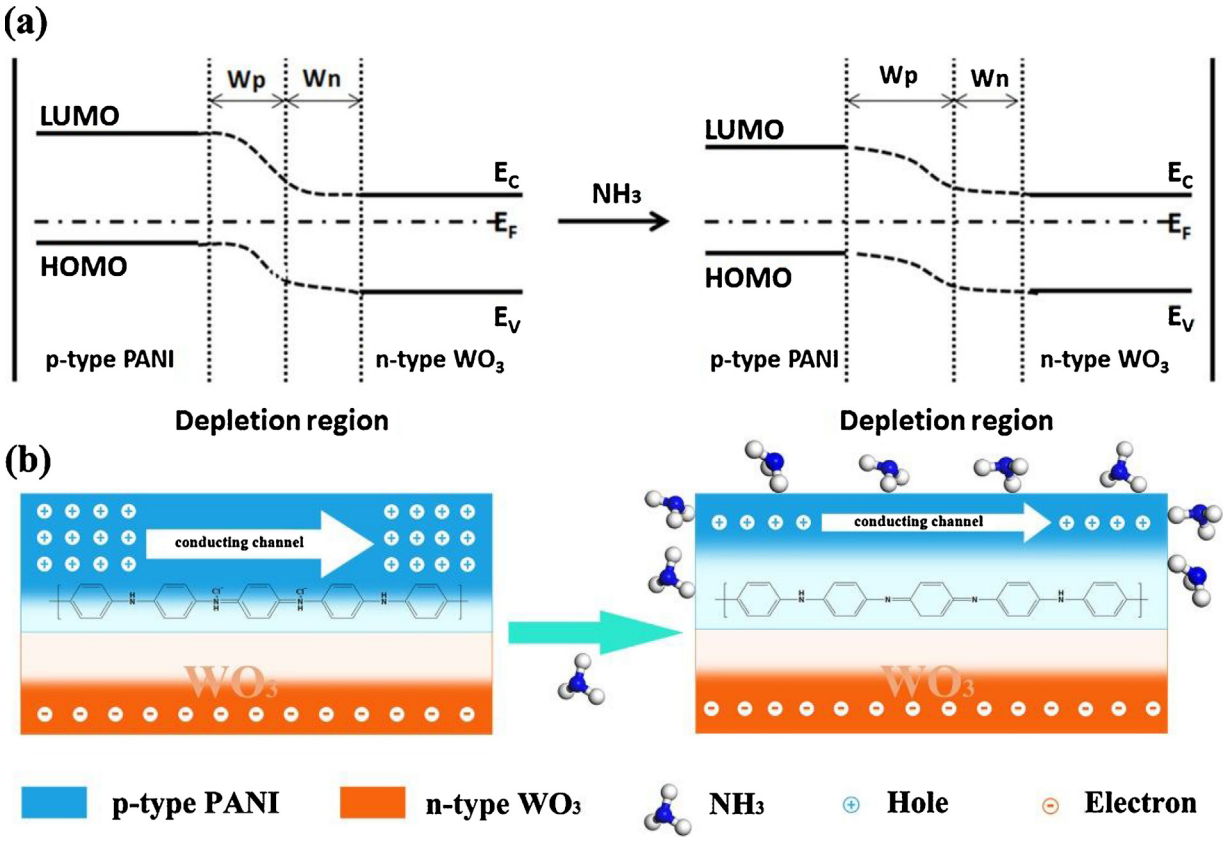

Fig. 12. (a) The energy band structure diagram of PANI@WO_3 hybrid in air and in NH_3; (b) Schematic illustration of sensing mechanism of PANI@WO_3 hybrid.

ered on flower-like WO_3 surface, the electrons in flower-like WO_3 and holes in PANI will diffuse in opposite direction because of the different Fermi energy (Fig. 12a). Finally, the *p-n* heterojunction in equilibrium and a narrow depletion area were formed at the heterointerface between PANI and flower-like WO_3 [29], as shown in Fig. 12(a, b). A wide conduction channel means a low resistance in PAW10 hybrid. When the PAW10 hybrid was exposed to NH_3 atmosphere, NH_3 withdrew the protons from acidified polyaniline and destroyed the original equilibrium state, resulting in the increase of PAW10 hybrid resistance. In this regard, the depletion layer area at heterointerface of PANI and flower-like WO_3 became thicker and the conduction channel became narrower, which induced the increase of resistance. Therefore, according to the response definition ($S = R_g/R_a$) for p-type semiconductor to electron-donating gas, the formation of *p-n* junction significantly improved the sensitivity.

4. Conclusions

In summary, a smart room temperature NH_3 sensor based on Polyaniline (PANI)@flower-like WO_3 nanocomposites loaded on flexible PET substrate was successfully developed by a facile and economical in situ chemical oxidation polymerization method. The gas sensing performance demonstrated that the sensor using PANI@10 mol% flower-like WO_3 nanocomposites is superior to other fabricated devices toward NH_3 at room temperature and the low detection limit was 500 ppb. The present sensor also exhibited admirable response and recovery rates, outstanding selectivity and moisture resistance. The excellent NH_3 sensing characteristics are owing to the distinctive morphology structure and the formation of *p-n* heterojunctions at the interfaces between PANI and flower-like WO_3. Furthermore, the PANI@flower-like WO_3 nanocomposites

can be a promising candidate material for fabricating flexible room temperature NH_3 sensor with the potential application value in area flexible electronic and wearable electronic devices.

Acknowledgements

This work is supported by the National Nature Science Foundation of China (Nos. 61327804, 61520106003, 61474057, 61503148 and 61473132), Program for Chang Jiang Scholars and Innovative Research Team in University (No. IRT13018) and National High-Tech Research and Development Program of China (863 Program, No. 2014AA06A505), Science and Technology Development Plan of Jilin Province (20140622005JC). National Key Research and Development Program of China (No. 2016YFC0207300).

Appendix A. Supplementary data

Supplementary data associated with this article can be found, in the online version, at https://doi.org/10.1016/j.snb.2017.11.081.

References

[1] B. Timmer, W. Olthuis, A. Berg, Ammonia sensors and their applications-a review, Sens. Actuators B: Chem. 107 (2005) 666–677.
[2] Q. Qi, T. Zhang, L. Liu, X. Zheng, G. Lu, Improved NH_3, C_2H_5OH, and CH_3COCH_3 sensing properties of SnO_2 nanofibers by adding block copolymer P123, Sens. Actuators B: Chem. 141 (2009) 174–178.
[3] P. Guo, H. Pan, Selectivity of Ti-doped In_2O_3 ceramics as an ammonia sensor, Sens. Actuators B: Chem. 114 (2006) 762–767.
[4] S. Zolghadr, K. Khojier, S. Kimiagar, Ammonia sensing properties of alpha-Fe_2O_3 thin films during post-annealing process, Procedia Mater. Sci. 11 (2015) 469–473.
[5] N. Dien, D. Tho, V. Hien, D. Vuong, N. Chien, ZnO nanoplates surfaced-decorated by WO_3 nanorods for NH_3 gas sensing application, Adv. Nat. Sci.: Nanosci. Nanotechnol. 7 (2016) 1–6.
[6] X. Liang, T. Zhong, H. Guan, F. Liu, G. Lu, B. Quan, Ammonia sensor based on NASICON and Cr_2O_3 electrode, Sens. Actuators B: Chem. 136 (2009) 479–483.
[7] F. Liu, R. Sun, Y. Guan, X. Cheng, H. Zhang, Y. Guan, X. Liang, P. Sun, G. Lu, Mixed-potential type NH_3 sensor based on stabilized zirconia and $Ni_3V_2O_8$ sensing electrode, Sens. Actuators B: Chem. 210 (2015) 795–802.
[8] W. Meng, L. Dai, J. Zhu, Y. Li, W. Meng, H. Zhou, A novel mixed potential NH_3 sensor based on TiO_2@WO_3 core-shell composite sensing electrode, Electrochim. Acta 193 (2016) 302–310.
[9] N. Du, H. Zhang, B. Chen, X. Ma, Z. Liu, J. Wu, Porous indium oxide nanotubes: layer-by-layer assembly on carbon-nanotube templates and application for room-temperature NH_3 gas sensors, Adv. Mater. 19 (2007) 1641–1645.
[10] Y. Lin, L. Huang, L. Chen, J. Zhang, L. Shen, Q. Chen, Fully gravure-printed NO_2 gas sensor on a polyimide foil using WO_3-PEDOT:PSS nanocomposites and Ag electrodes, Sens. Actuators B: Chem. 216 (2015) 176–183.
[11] Y. Li, H. Zhao, H. Ban, M. Yang, Composites of Fe_2O_3 nanosheets with polyaniline: preparation, gas sensing properties and sensing mechanism, Sens. Actuators B: Chem. 245 (2017) 34–43.
[12] L. Wang, H. Huang, S. Xiao, D. Cai, Y. Liu, B. Liu, Enhanced sensitivity and stability of room-temperature NH_3 sensors using core-shell CeO_2 nanoparticles@cross-linked PANI with p-n heterojunctions, ACS Appl. Mater. Interfaces 6 (2014) 14131–14140.
[13] Q. Nie, Z. Pang, H. Lu, Y. Cai, Q. Wei, Ammonia gas sensors based on In_2O_3/PANI hetero-nanofibers operating at room temperature, Beilstein J. Nanotechnol. 7 (2016) 1312–1321.
[14] S. Kulkarni, Y. Navale, S. Navale, N. Ramgir, A. Debnath, S. Gadkari, Enhanced ammonia sensing characteristics of tungsten oxide decorated polyaniline hybrid nanocomposites, Org. Electron. 45 (2017) 65–73.
[15] T. Wang, Y. Guo, P. Wan, H. Zhang, X. Chen, X. Sun, Flexible transparent electronic gas sensors, Small 12 (2016) 3478–3756.
[16] S. Bai, C. Sun, P. Wan, C. Wang, R. Luo, Y. Li, Transparent conducting films of hierarchically nanostructured polyaniline networks on flexible substrates for high-performance gas sensors, Small 11 (2015) 306–310.
[17] Y. Long, L. Zhang, Y. Ma, Z. Chen, N. Wang, Z. Zhang, Electrical conductivity of an individual polyaniline nanotube synthesized by a self-assembly method, Macromol. Rapid Commun. 24 (2003) 938–942.
[18] S. Kuchibhatla, A. Karakoti, D. Bera, S. Seal, One dimensional nanostructured materials, Prog. Mater. Sci. 52 (2007) 699–913.
[19] C. Wang, R. Sun, X. Li, Y. Sun, P. Sun, F. Liu, Hierarchical flower-like WO_3 nanostructures and their gas sensing properties, Sens. Actuators B: Chem. 204 (2014) 224–230.
[20] Y. Wang, J. Liu, X. Cui, Y. Gao, J. Ma, Y. Sun, NH_3 gas sensing performance enhanced by Pt-loaded on mesoporous WO_3, Sens. Actuators B: Chem. 238 (2017) 473–481.
[21] C. Wang, L. Wang, J. Jin, J. Liu, Y. Li, M. Wu, Probing effective photocorrosion inhibition and highly improved photocatalytic hydrogen production on monodisperse PANI@CdS core-shell nanospheres, Appl. Catal. B 188 (2016) 351–359.
[22] L. Xue, W. Wang, Y. Guo, G. Liu, P. Wan, Flexible polyaniline/carbon nanotube nanocomposite film-based electronic gas sensors, Sens. Actuators B: Chem. 244 (2017) 47–53.
[23] S. Bai, Y. Zhao, J. Sun, Z. Tong, R. Luo, D. Li, A. Chen, Preparation of conducting films based on α-MoO_3/PANI hybrids and their sensing properties to triethylamine at room temperature, Sens. Actuators B: Chem. 239 (2017) 131–138.
[24] A. Mane, S. Navale, S. Sen, D. Aswal, S. Gupta, V. Patil, Nitrogen dioxide (NO_2) sensing performance of p-polypyrrole/n-tungsten oxide hybrid nanocomposites at room temperature, Org. Electron. 16 (2015) 195–204.
[25] L. Quan, J. Sun, S. Bai, R. Luo, D. Li, A. Chen, A flexible sensor based on polyaniline hybrid using ZnO as template and sensing properties to triethylamine at room temperature, Appl. Surf. Sci. 399 (2017) 583–591.
[26] M. Kotal, A. Hakur, A. Bhowmick, Polyaniline-carbon nanofiber composite by a chemical grafting approach and its supercapacitor application, ACS Appl. Mater. Interfaces 5 (2013) 8374–8386.
[27] G. Gaikwad, P. Patil, D. Patil, J. Naik, Synthesis and evaluation of gas sensing properties of PANI based graphene oxide nanocomposites, Mater. Sci. Eng. B 218 (2017) 14–22.
[28] S. Bai, Y. Tian, M. Cui, J. Sun, Y. Tian, R. Luo, Polyaniline@SnO_2 heterojunction loading on flexible PET thin film for detection of NH_3 at room temperature, Sens. Actuators B: Chem. 226 (2016) 540–547.
[29] H. Tai, Y. Jiang, G. Xie, J. Yu, X. Chen, Fabrication and gas sensitivity of polyaniline-titanium dioxide nanocomposite thin film, Sens. Actuators B: Chem. 125 (2007) 644–650.
[30] G. Khuspe, D. Bandgar, S. Sen, V. Patil, Fussy nanofibrous network of polyaniline (PANi) for NH_3 detection, Synth. Met. 162 (2012) 1822–1827.
[31] C. Liu, H. Tai, P. Zhang, Z. Ye, Y. Su, Y. Jiang, Enhanced ammonia-sensing properties of PANI-TiO_2-Au ternary self-assembly nanocomposite thin film at room temperature, Sens. Actuators B: Chem. 246 (2017) 85–95.
[32] D. Bandgar, S. Navale, Y. Navale, S. Ingole, F. Stadler, N. Ramgir, Flexible camphor sulfonic acid-doped PAni/α-Fe_2O_3 nanocomposite films and their room temperature ammonia sensing activity, Mater. Chem. Phys. 189 (2017) 191–197.
[33] I. Jimenez, A. Vila, A. Calveras, J. Morante, Gas-sensing properties of catalytically modified WO_3 with copper and vanadium for NH_3 detection, IEEE Sens. J. 5 (2005) 385–391.
[34] V. Nguyen Minh, T. Tran Nam, H. Truong Thi, C. Nguyen Duc, Q. Nguyen Duc, D. Lee, Ni_2O_3 decoration of WO_3 thin film for high sensitivity NH_3 gas sensor, Mater. Trans. 56 (2015) 1354–1357.
[35] H. Hien, T. Giang, N. Hieu, T. Trung, C. Tuan, Elaboration of Pd-nanoparticle decorated polyaniline films for room temperature NH_3 gas sensors, Sens. Actuators B: Chem. 249 (2017) 348–356.

Biographies

Siqi Li received her M.S. degree from department of Chemical Engineering and Technology, Harbin Engineering University, China in 2016. Now, she is studying for her Ph.D. degree in College of Electronic Science and Engineering, Jilin University, China. She is engaged in the synthesis and characterization of organic/inorganic hybrid nanomaterials for gas sensor and development of flexible device.

Pengfei Lin received the B. Eng. degree in department of electronics and information engineering, Jilin University, in 2015. And he entered his M.S. course in College of Electronic Science in 2016. Now, he is studying for his M.S. degree, majored in the gas sensor system and the Internet of things.

Liupeng Zhao received the B. Eng. degree in department of electronic sciences and technology, Jilin University, in 2016. At the same year, he entered his M.S. course in College of Electronic Science. Now, he is studying for his M.S. degree, majored in the synthesis and characterization of the semiconducting functional materials and gas sensors.

Chong Wang received the B. Eng. degree in department of electronic sciences and technology, Jilin University, in 2013. At the same year, she entered her M.S. course in College of Electronic Science. Now, she is studying for her Ph.D. degree, majored in the synthesis and characterization of the semiconducting functional materials and gas sensors.

Deye Liu received the B.Eng. degree in department of electronic science and technology in 2015. He is currently studying for his M.E. Sci. degree in College of Electronic Science and Engineering, Jilin University, China.

Fangmeng Liu received his Ph.D. degree in 2017 from College of Electronic Science and Engineering, Jilin University, China. Now he is a lecturer of Jilin University, China. His current research interests include the application of funtional materials and development of solid state electrolyte gas sensor and flexible device.

Peng Sun received his Ph.D. degree from Jilin University of China in 2014. Now, he is engaged in the synthesis and characterization of the semiconducting functional materials and gas sensors.

Xishuang Liang received the B. Eng. degree in Department of Electronic Science and Technology in 2004. He received his Doctor's degree in College of Electronic Science and Engineering at Jilin University in 2009. Now he is an professor of Jilin University, China. His current research is solid electrolyte gas sensor.

Fengmin Liu received the B.E. degree in Department of Electronic Science and Technology in 2000. She received her Doctor's degree in College of Electronic Science and Engineering at Jilin University in 2005. Now she is an professor in Jilin University, China. Her current research is preparation and application of semiconductor oxide, especial in gas sensor and solar cell.

Xu Yan received his M.S degree in 2013 from Nanjing Agricultural University. He joined the group of Prof. Xingguang Su at Jilin University and received his Ph.D. degree in June 2017. Since then, he did postdoctoral work with Prof. Geyu Lu. Currently, his research interests mainly focus on the development of the functional nanomaterials for chem/bio sensors.

Yuan Gao received her PhD degree from Department of Analytical Chemistry at Jilin University in 2012. Now she is an associate professor in Jilin University, China. Her current research is focus on the preparation and application of graphene and semiconductor oxide, especial in gas sensor and biosensor.

Geyu Lu received the B.S. degree in electronic sciences in 1985 and the M.S. degree in 1988 from Jilin University in China and the D.Eng degree in 1998 from Kyushu University in Japan. Now he is a professor of Jilin University, China. Now, he is interested in the development of functional materials and chemical sensors.